

# Hyperuniformity in Ashkin-Teller model

Indranil Mukherjee and P. K. Mohanty

Department of Physical Sciences, Indian Institute of Science Education and Research  
Kolkata, Mohanpur, 741246 India.

E-mail: [pkmohanty@iiserkol.ac.in](mailto:pkmohanty@iiserkol.ac.in)

**Abstract.** We show that equilibrium systems in  $d$  dimension that obey the inequality  $d\nu > 2$ , known as Harris criterion, exhibit suppressed energy fluctuation in their critical state. Ashkin-Teller model is an example in  $d = 2$  where the correlation length exponent  $\nu$  varies continuously with the inter-spin interaction strength  $\lambda$  and exceeds the value  $\frac{d}{2}$  set by Harris criterion when  $\lambda$  is negative; there, the variance of the subsystem energy across a length scale  $l$  varies as  $l^{d-\alpha}$  with hyperuniformity exponent  $\alpha = 2(1 - \nu^{-1})$ . Point configurations constructed by assigning unity to the sites which has coarse-grained energy beyond a threshold value also exhibit suppressed number fluctuation and hyperuniformity with same exponent  $\alpha$ .

## 1. Introduction

Hyperuniform systems are exotic states of matter that lie between crystal and liquid [1, 2]. In small length scales they appear disordered whereas at large-scales they are like perfect crystals with minimal or no density fluctuations. Instances of hyperuniformity are observed in numerous natural systems –arrangement of photo receptors in birds [3, 4, 5], fish [6] and other vertebrates [7], vegetation of ecosystems [8, 9], and human settlements [10]. Materials like amorphous silica [11], superconducting vortex lattices [12], amorphous ice [13] binary-mixture of charged colloids [14, 15] exhibit hyperuniform structure. Many models of two-phase co-existence [16, 17, 18, 19], self organized critical states of sand-pile models [20, 9] and other critical absorbing states [21, 22, 23, 24, 25] also exhibit hyperuniformity in their critical state. Strangely, patterns in prime numbers [26, 27] maximally packed extended objects [28, 29], quasi-crystals in general [30, 31] and several synthetic materials [32, 33, 34] adds to the class of hyperuniform systems.

A general mechanism that leads to stable hyperuniform structures is yet to be found, although some attempts have been made in specific systems [35, 36].

### 1.1. What is hyperuniformity

In point configurations, hyperuniformity is defined as follows. Let us consider a  $L^d$  box containing  $M$  particles in total, distributed homogeneously, so that the density of the system is  $\rho = M/L^d$ . Then, any subsystem of volume  $V = R^d$  is expected to have  $\rho V$  number of particles on average, but the actual number of particles  $N$  in the subsystem in any instance would deviate from the expected value and it is quantified by the variance  $\sigma^2(V) = \langle (N - \rho V)^2 \rangle = \langle N^2 \rangle - \langle N \rangle^2$ . Since  $N$  is a sum of random variables  $s(\Delta V)$  which takes integer values 1,0 depending on whether a particle is present or absent in volume element  $\Delta V$ . The law of large numbers then dictates the variance  $\sigma^2(V)$  to be proportional to  $V$  [37]. This is generically true in many physical systems where the variance of an observable need to be additive so that corresponding susceptibility  $\sigma^2(V)/V$  in the thermodynamic limit becomes a intensive variable. However there are exceptions, where  $\sigma^2(V) \sim V^q$  with  $q < 1$ , i.e.,

$$\sigma^2(R) \sim R^{d-\alpha}, \quad (1)$$

where  $d(1 - q) = \alpha$ . These systems are called hyperuniform as the density fluctuations of the system vanishes in the  $V \rightarrow \infty$  limit. In small length scales hyperuniform systems behaves like a gas (disordered), whereas their large-scale properties are crystal like (ordered). The hyperuniformity exponent  $0 < \alpha < 1$  characterizes the degree of hyperuniformity. In fact, Eq. (1) is formally known as Class-III hyperuniformity (the classification of hyperuniformity is discussed in Ref. [1]).

### 1.2. Hyperuniform critical states

Hyperuniformity can occur in equilibrium systems that undergo a continuous phase transition when an external tuning parameter crosses a critical threshold. During the

phase transition, the order parameter  $\phi$  of a thermodynamically large system vanishes in the disordered phase and it picks up a nonzero values in the ordered phase. At the critical point, the system exhibits scale-invariance as the correlation length  $\xi$  diverges there:  $\xi \sim |\Delta|^{-\nu}$ , where  $\Delta$  measures the deviation of the tuning parameter from its critical value ( $\Delta > 0$  in ordered phase). The mean and the variance of the order parameter scales as

$$\langle \phi \rangle \sim \Delta^\beta; \quad \langle \phi^2 \rangle - \langle \phi \rangle^2 \sim |\Delta|^{-\gamma}. \quad (2)$$

Again, in a homogeneous and isotropic system, the two point correlation of  $\phi$  separated by a distance  $|\mathbf{r}|$  is defined by

$$c(\mathbf{r}) = \langle \phi(\mathbf{x})\phi(\mathbf{x} + \mathbf{r}) \rangle - \langle \phi(\mathbf{x}) \rangle \langle \phi(\mathbf{x} + \mathbf{r}) \rangle \sim \frac{e^{-|\mathbf{r}|/\xi}}{|\mathbf{r}|^{d-2+\eta}}. \quad (3)$$

Clearly  $c(\mathbf{r})$  is scale-invariant at the critical point where  $\xi \rightarrow \infty$ . The set of critical exponents  $\{\nu, \beta, \gamma, \eta\}$  defines a universality class. They depend only on the dimension of the system and the symmetry of the order parameter which is broken at the critical point; other microscopic details are irrelevant. The exponents are not all independent they are related by scaling relations [38],

$$2\beta + \gamma = d\nu; \quad 2 - \eta = \frac{\gamma}{\nu}. \quad (4)$$

Following the work by Ornstein-Zernike [39, 40] one can define a total correlation function  $h(\mathbf{r})$ , similar to that of liquids in equilibrium [41, 42],

$$h(\mathbf{r}) = c(\mathbf{r}) + \langle \phi \rangle \int_{L^d} c(\mathbf{r} - \mathbf{r}')h(\mathbf{r}')d\mathbf{r}'. \quad (5)$$

The first term in the right hand side corresponds to the direct correlation function of observables separated by distance  $\mathbf{r}$  and the second one captures the indirect contribution coming to these points through another point at a distance  $\mathbf{r}'$ . Let the Fourier transform of  $c(\mathbf{r})$  and  $h(\mathbf{r})$  be  $\tilde{c}(\mathbf{k})$  and  $\tilde{h}(\mathbf{k})$ . Since, a Fourier transform of the integral in the right hand side is a convolution, we get  $\tilde{h}(\mathbf{k}) = \tilde{c}(\mathbf{k})/1 - \langle \phi \rangle \tilde{c}(\mathbf{k})$ . The usual structure factor [42] is then

$$S(\mathbf{k}) = 1 + \langle \phi \rangle \tilde{h}(\mathbf{k}) = \frac{1}{1 - \langle \phi \rangle \tilde{c}(\mathbf{k})}. \quad (6)$$

At the critical point,  $c(\mathbf{r}) \sim |\mathbf{r}|^{-d+2-\eta}$  and thus  $c(\mathbf{k}) \sim -|\mathbf{k}|^{\eta-2}$ . From the scaling relations, we get  $\eta = 2 - d + 2\frac{\beta}{\nu} = 2 - \frac{\gamma}{\nu}$ ; since critical exponents  $\beta, \gamma, \nu$  are positive,  $\eta$  is bounded in the range  $(2 - d, 2)$ . Thus,  $c(\mathbf{k})$  diverges in the the small  $|\mathbf{k}|$  limit, we have

$$S(\mathbf{k}) \sim |\mathbf{k}|^\alpha \quad \text{with } \alpha = \frac{\gamma}{\nu} = 2 - \eta = d - 2\frac{\beta}{\nu}. \quad (7)$$

In fact, the above relation is also considered as definition of hyperuniformity equivalent to Eq. (1) with exponent  $\alpha$  [1]. A system is hyperuniform when the structure factor  $S(\mathbf{k}) \sim |\mathbf{k}|^\alpha$  with  $\alpha > 0$ . In effect  $S(\mathbf{k})$  of hyperuniform systems vanishes as  $|\mathbf{k}| \rightarrow 0$ . Based on this, hyperuniformity is classified into three categories -

$$\text{Class I } (\alpha > 1) \quad : \quad \sigma^2(R) \sim R^{d-1}$$

$$\begin{aligned}
\text{Class II } (\alpha = 1) & : \sigma^2(R) \sim R^{d-1} \ln(R) \\
\text{Class III } (0 < \alpha < 1) & : \sigma^2(R) \sim R^{d-\alpha}
\end{aligned} \tag{8}$$

Hyperuniform critical states generally belong to **Class III** [1], the weakest among the three classes.

Hyperuniformity is not restricted to equilibrium. Recent works indicate that, under nonequilibrium conditions, two-dimensional crystals exhibit hyperuniformity [44]. In absorbing phase transition, the sub-critical phase is non-fluctuating. The system approach the absorbing state by pushing particles from active local regions to their neighbourhood, thereby reducing density fluctuations - or creating hyperuniformity locally. This process happens over a finite distance (the correlation length  $\xi$ ) and it extends all over the system as the critical point is approached ( $\xi \rightarrow \infty$ ). In fact, critical absorbing states are generically hyperuniform [22]. In Manna sand-pile model, at the critical density  $\rho_c$  the density fluctuation  $\sigma^2(l) = \langle \rho(l)^2 \rangle - \langle \rho(l) \rangle^2$  in a volume  $V = l^d$  is found to be,

$$\sigma^2(l) = \langle \rho(l)^2 \rangle - \langle \rho(l) \rangle^2 \sim l^{d-\alpha} \tag{9}$$

with  $\alpha = 0.425, 0.45, 0.24$  respectively for  $d = 1, 2, 3$  [22]. Direct measurement of structure factor also confirm that  $S(k) \sim k^\alpha$  with same  $\alpha$  value. This work by Hexner and Levin [22] also showed that, within the acceptable error limits, the hyperuniformity exponent  $\alpha$  matches with  $2-\eta$ , where  $\eta$  is the exponent related to the correlation function of activity density  $\rho_a$  at the critical point, i.e.,  $\langle \rho_a(\mathbf{x})\rho_a(\mathbf{x} + \mathbf{r}) \rangle - \langle \rho_a(\mathbf{x}) \rangle \langle \rho_a(\mathbf{x} + \mathbf{r}) \rangle \sim |\mathbf{r}|^{-d+2-\eta}$ . In fact, an exceptionally uniform density profile was observed earlier [21] in one dimensional Manna models [43], though it was not named as hyperuniformity; the exponent  $\alpha \equiv d - 2\frac{\beta}{\nu} = 0.496$  (calculated using  $\beta, \gamma$  as that of directed percolation [45]) is quite close to  $\alpha = 0.425$  obtained in Ref. [22]. The discrepancy owes to the fact that (a) there are strong finite size effects and (b) the system takes unusually long time to reach its correct steady state where density profile is hyperuniform [21].

Other models having absorbing phase transition like Oslo model [46, 47], conserved lattice gas [48], random organization (RO) models [49], and facilitated exclusion process [50] also exhibit hyperuniformity, which is reported in Refs. [24], [23], and [25] respectively. For a recent review on hyperuniformity in non-equilibrium systems, see Ref. [51].

### 1.3. Objective of our study

In this article we explore another possibility where internal energy of the system, at its critical point, exhibit hyperuniform distribution. In  $2^{nd}$  order equilibrium phase transitions, the average of energy of the system vary continuously across the critical point but the variance, known as the specific heat  $C_v$  diverges,

$$C_v = \frac{1}{V} (\langle E^2 \rangle - \langle E \rangle^2) \sim \Delta^{-a}. \tag{10}$$

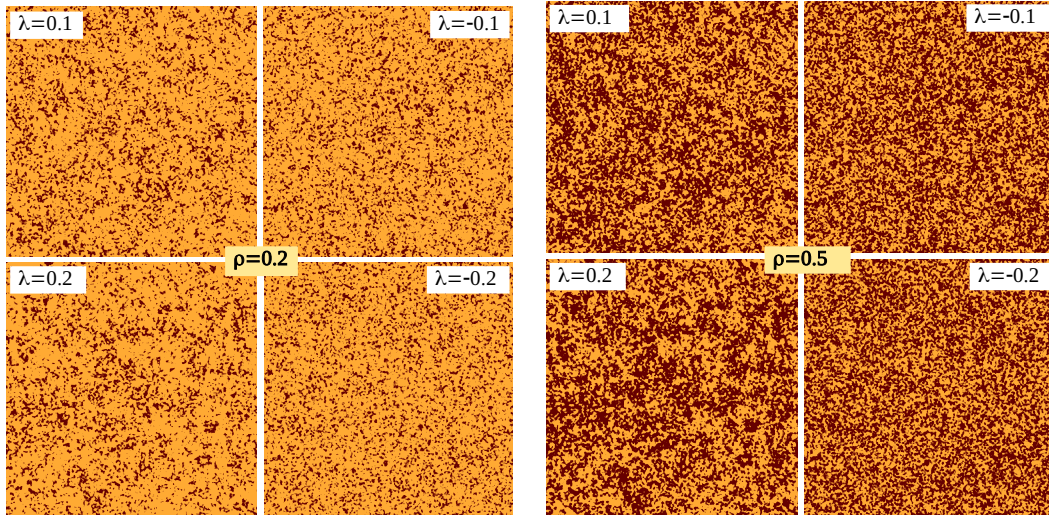


**Figure 1.** Point configurations generated in Ashkin Teller model by assigning, 1 (dark colour) to sites whose energy exceeds a pre-determined threshold, else 0 (light colour) on a  $1024 \times 1024$  square lattice. Configurations with negative  $\lambda$  (hyperuniform) are compared with those having positive values (uniform) for particle density is  $\rho = 0.2$  (left),  $0.5$  (right).

Here we denote the specific heat exponent as  $a$  (as hyperuniformity exponent is usually denoted as  $\alpha$  in recent literature). In a finite system, the correlation length  $\xi$  is limited by the system size  $L$  and thus  $\Delta \sim L^{-1/\nu}$ , resulting in

$$\sigma_E^2(L) = \langle E^2 \rangle - \langle E \rangle^2 \sim L^{d+\frac{a}{\nu}}. \quad (11)$$

Energy  $E_l$  of a large subsystem of size  $l \times l$ , with  $1 \ll l \ll L$  is expected to show a similar scaling behaviour,

$$\sigma_{E_l}^2(l) = \langle E_l^2 \rangle - \langle E_l \rangle^2 \sim l^{d+\frac{a}{\nu}}. \quad (12)$$

A comparison with Eq. (1) gives us  $\alpha = -\frac{a}{\nu}$ . Since hyperuniformity distribution is possible only for  $0 < \alpha < 1$ , we need  $-1 < \frac{a}{\nu} < 0$ . Is it possible? Usually, the specific heat of a system diverges at the critical point, which corresponds to  $a > 0$  and  $a$  is positive. We consider Ashkin-Teller model in 2d as an example, where  $a$  can become negative in some regime of the parameter space. There we show that, energy of a subsystem exhibit hyperuniformity with

$$\alpha = \frac{|a|}{\nu} = 2(1 - \nu^{-1}), \quad (13)$$

where in the last step we use the scaling relation  $2 - a = d\nu$ .

Hyperuniformity is primarily studied in systems which are described by point configurations. To substantiate, we use a threshold filter that converts the real variable  $E_l$  to integers 1, 0 representing presence and absence of particles, and thereby generates point configurations. Although mean density of these point configurations depend on the threshold, we find that the fluctuations exhibit hyperuniformity with exponent  $\alpha$

that does not depend on particle density.  $\alpha$  is given by Eq. (13). In Fig. 1 we represent the point configurations of the Ashkin-Teller model pictorially for interaction strengths  $\lambda = \pm 0.1, \pm 0.2$  and two different particle densities  $\rho = 0.2$ (left), 0.5 (right). The dark colour there represent occupied sites. Clearly, configurations with negative  $\lambda$  appears smoother. Details are discussed in the following section.

## 2. Ashkin-Teller Model

Ashkin Teller (AT) model [52, 53, 54, 55] is a two-layer Ising system defined on a  $L \times L$  square lattice with periodic boundary conditions in both directions. The sites of the lattice with coordinates  $(x, y)$  is represented by vectors  $\mathbf{i} \equiv (x, y)$  where  $x, y = 1, 2, \dots, L$ . Each site  $\mathbf{i}$  of the lattice carries two different Ising spins  $\sigma_{\mathbf{i}} = \pm$  and  $\tau_{\mathbf{i}} = \pm$  which interact as follows.

$$H = -J \sum_{\langle \mathbf{ij} \rangle} \sigma_{\mathbf{i}} \sigma_{\mathbf{j}} - J \sum_{\langle \mathbf{ij} \rangle} \tau_{\mathbf{i}} \tau_{\mathbf{j}} - \lambda \sum_{\langle \mathbf{ij} \rangle} \sigma_{\mathbf{i}} \sigma_{\mathbf{j}} \tau_{\mathbf{i}} \tau_{\mathbf{j}}. \quad (14)$$

Here  $\langle \mathbf{ij} \rangle$  denotes a pair of nearest-neighbor sites,  $J$  is the strength of intra-spin interactions and  $\lambda$  represents interactions among  $\sigma$  and  $\tau$  spins. The energy of the system in Eq. (14) remains unchanged under one or more of the the following transformations:

$$\sigma \rightarrow -\sigma; \quad \tau \rightarrow -\tau; \quad \sigma \rightarrow \tau. \quad (15)$$

Thus it is natural to consider that the quantities  $M = \langle \sigma \rangle = \langle \tau \rangle$ , and  $P = \langle \sigma \tau \rangle$  which obey these symmetries may break giving rise to an ordered phase. Formally these observable are referred to as magnetisation and polarisation respectively. In AT model, both  $M$  and  $P$  break the symmetry across the self-dual critical line [56],

$$T_c = 1, \lambda_c = \lambda, J_c = \frac{1}{2} \sinh^{-1}(e^{-2\lambda}) \quad (16)$$

and generate finite magnetization ( $M \neq 0$ ) and finite polarization ( $P \neq 0$ ) simultaneously. The electric and magnetic phase transitions are characterized by the respective critical exponents (denoted by subscripts  $e, m$  respectively)

$$\begin{aligned} \langle M \rangle &\sim \Delta^{\beta_m}; \quad \chi_m = \langle M^2 \rangle - \langle M \rangle^2 \sim \Delta^{-\gamma_m}; \\ \langle P \rangle &\sim \Delta^{\beta_e}; \quad \chi_e = \langle P^2 \rangle - \langle P \rangle^2 \sim \Delta^{-\gamma_e}; \end{aligned} \quad (17)$$

where  $\Delta = T_c - T$ . The other critical exponents  $\nu, a$  associated with the correlation length and the specific heat respectively, do not depend on the order parameters and thus carry no subscripts,

$$\xi \sim \Delta^{-\nu}; \quad C_v = \frac{1}{L^2} (\langle E^2 \rangle - \langle E \rangle^2) \sim \Delta^{-a}. \quad (18)$$

The Ashkin-Teller model can be mapped to the eight vortex model introduced and solved by Baxter [57, 55]. This mapping and re-normalization group arguments [53] provide exact value of the critical exponents in terms of  $\mu = \cos^{-1}(e^{2\lambda} \sinh(2\lambda))$ ,

$$\nu = \frac{2(\mu - \pi)}{4\mu - 3\pi}; \quad a = 2(1 - \nu); \quad \beta_e = \frac{2\nu - 1}{4}; \quad \gamma_e = \frac{1}{2} + \nu; \quad \beta_m = \frac{\nu}{8}; \quad \gamma_m = \frac{7\nu}{4}. \quad (19)$$

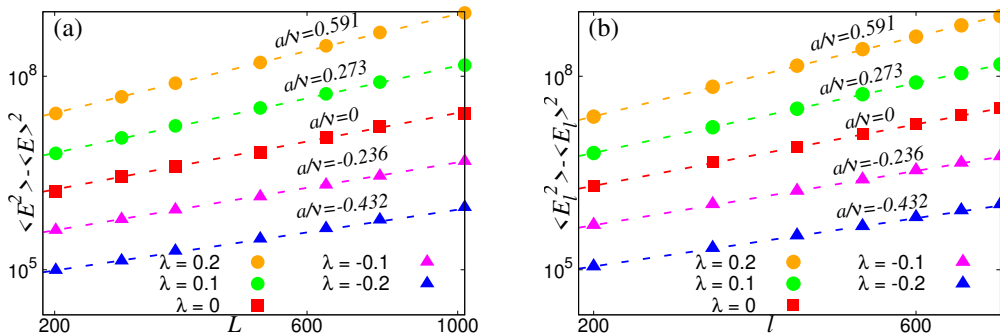


**Figure 2.** (a) Log-scale plot of variance of total energy  $\langle E^2 \rangle - \langle E \rangle^2$  as a function of system size  $L$  for different  $\lambda$  values (symbols) are compared with  $L^{d+\frac{a}{\nu}}$  (dashed lines). (b) Energy fluctuations in  $l \times l$  subsystems:  $\langle E_l^2 \rangle - \langle E_l \rangle^2$  as a function of  $l$  in log-scale for different  $\lambda$  values (symbols) matches with dashed lines  $l^{d+\frac{a}{\nu}}$  where  $a$  is given by Eq. (19). In all cases  $L = 1024$ , and averaging is done over more than  $10^6$  samples; data are also scaled by factors  $\{\frac{1}{2}, 1, 2, 4, 8\}$  (bottom to top) for better visibility.

Note that the critical exponents of magnetic transition satisfy the following relations:  $\frac{\beta_m}{\nu} = \beta_m^0$ ,  $\frac{\gamma_m}{\nu} = \gamma_m^0$ , where  $\{\beta_m^0 = \frac{1}{8}, \gamma_m^0 = \frac{7}{4}\}$  are the critical exponents of Ising universality class in  $d = 2$ . This is the well-known weak universality scenario proposed by Suzuki [58], and observed in several experiments [59, 60]. According to weak-universality hypothesis, universality feature of a phase transition should be determined on how the physical quantities depend on the correlation length  $\xi$  which is an emerging property of the system, not on  $\Delta = T_c - T$  because  $T_c$  is a non-universal – it depends on the microscopic details of the system.

The electric transition violates both universality and weak-universality hypothesis; all its critical exponents vary continuously with  $\lambda$ . Recent works propose a super universality hypothesis [61] which states the following. Critical behaviour of a system form a super-universality class when the scaling function that relates the binder cumulant of the system with the second moment correlation length in units of system size  $L$  remains invariant along the critical line, even when the critical exponents vary. It turns out that both magnetic and electric phase transition of AT model belong to Ising-super-universality class [61].

### 2.1. Energy distribution

In this article we focus on studying energy distribution along the critical line. In a finite system, the correlation length  $\xi$ , which is supposed to diverge as  $\Delta^{-\nu}$ , is bounded by the system size  $L$  and thus  $L \equiv \Delta^{-\nu}$ . Then,

$$\langle E^2 \rangle - \langle E \rangle^2 \sim L^d \Delta^{-\alpha} = L^{d+\frac{a}{\nu}}. \quad (20)$$

In Fig. 2(a) we have plotted  $\langle E^2 \rangle - \langle E \rangle^2$  as a function of system size  $L$  in log-scale, for different  $\lambda$ ; for comparison, dashed lines with slope  $d + \frac{a}{\nu}$  are drawn along the symbols. It is no surprise that they agree well.

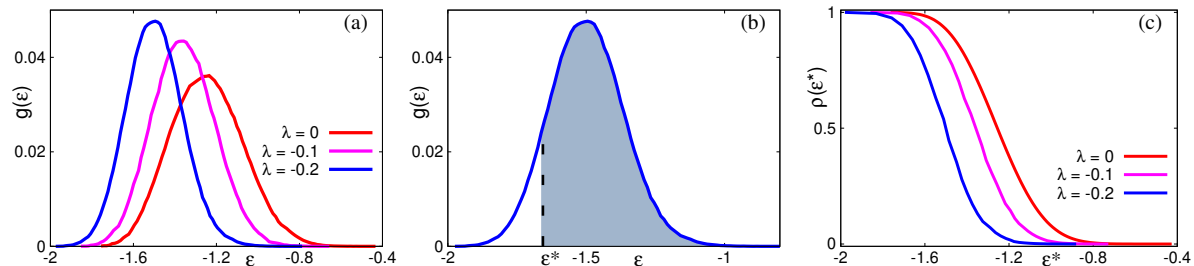


**Figure 3.** (a) The distribution  $g(\epsilon)$  of coarse-grained local energy  $\epsilon$  defined in Eq. (22) with  $l = 8$ . Different curves corresponds to  $\lambda = -0.2, -0.1, 0$ . (b) Schematic representation of particle density  $\rho(\epsilon^*)$ , as in Eq. (23). The shaded represents particle density. (c)  $\rho(\epsilon^*)$  as a function of the threshold  $\epsilon^*$  for  $\lambda = -0.2, -0.1, 0$ .

We now look at the energy of the subsystems of size  $l \times l$ , where  $l \ll L$ . First let us define the local energy at each site,

$$H_{\mathbf{i}} \equiv H_{x,y} = -J s_{x,y} (s_{x,y+1} + s_{x+1,y}) - J \tau_{x,y} (\tau_{x,y+1} + \tau_{x+1,y}) - \lambda (s_{x,y} \tau_{x,y} (s_{x,y+1} \tau_{x,y+1} + s_{x+1,y} \tau_{x+1,y})) \quad (21)$$

so that the total energy given in Eq. (14)  $H = \sum_{\mathbf{i}} H_{\mathbf{i}}$ . The homogeneity of the system states that  $\langle H \rangle = L^2 \langle H_{\mathbf{i}} \rangle$ . Energy of a subsystem of size  $l \times l$  is defined as  $E_l = \sum_{\mathbf{i} \in l \times l} H_{\mathbf{i}}$ , where the  $l \times l$  square is placed on the lattice such that its sides are aligned and one of its corner matched with a randomly chosen site  $\mathbf{j}$ . Clearly,  $\langle E_l \rangle = l^2 \langle H_{\mathbf{i}} \rangle$ . The variance of  $E_l$ ,  $\sigma_{E_l}^2(l) = \langle E_l^2 \rangle - \langle E_l \rangle^2$ , is calculated from Monte Carlo simulations when the system is in steady state. In Fig. 2(b) we plot  $\sigma_{E_l}^2(l)$  as a function of  $l$  in log-scale for different  $\lambda$ . Along with the data (symbols), for comparison, we draw dashed lines of slope  $d + \frac{a}{\nu}$ . A good match suggests that the subsystem energy fluctuation also obey the scaling  $\sigma_{E_l}^2(l) \sim l^{d + \frac{a}{\nu}}$ , similar to Eq. (20). Thus, the variance of subsystem energy also exhibit hyperuniformity when  $a < 0$ , i.e. when  $\lambda < 0$ .

## 2.2. Hyperuniformity in point configurations

Hyperuniformity is generally defined on point configurations carrying discrete variables on lattice or in continuum. Their pictorial representations are visually appealing as discrete variables generates sharp contrast – hyperuniform systems appears strikingly different and more uniform than their counterparts where particles are distributed randomly. Local energy  $H_{\mathbf{i}}$ , being a real variable, cannot display such a contrast. In the following we try to construct point configurations that faithfully represent the local energy. This can be done using a threshold energy  $\epsilon^*$  that places a point (particle) at every site  $(x, y)$  with energy  $H_{x,y}$  larger than  $\epsilon^*$ ; the particle density  $\rho$  of the point configurations can be controlled by varying  $\epsilon^*$ . This process does generate point configurations, but  $\rho(\epsilon^*)$  is limited to certain fixed values. This limitation arises because the local energy  $H_{x,y}$  in Eq. (21) is a discrete set (sum of integer multiples of  $J$  and  $\lambda$ ). To achieve a continuous variation of  $\rho$ , we need a coarse-grained energy at each site.

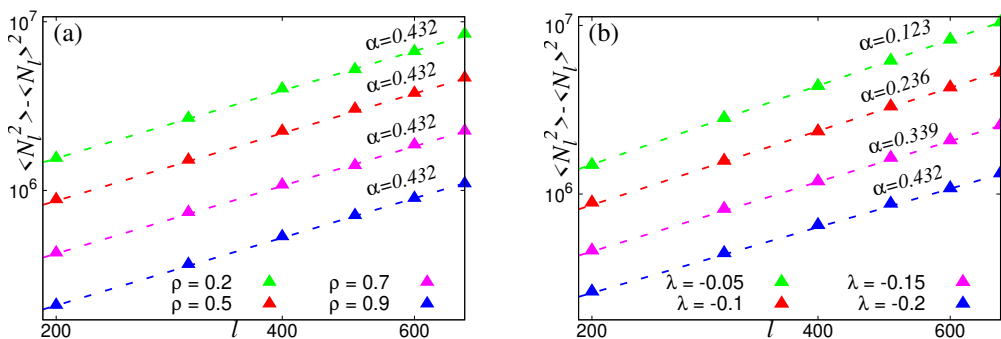


**Figure 4.** Log-scale plot of number fluctuations in  $l \times l$  subsystems  $\langle N_l^2 \rangle - \langle N_l \rangle^2$  as a function of  $l$ . (a)  $\lambda = -0.2$  and densities  $\rho = 0.2, 0.5, 0.7, 0.9$ . Dashed lines corresponds to  $l^{d-\alpha}$  with  $\alpha = \frac{|a|}{\nu} = 0.432$ , known exactly from Eq. (19). (b)  $\rho = 0.5$  and  $\lambda = -0.05, -0.1, -0.15, -0.2$ . Data (in symbols) are compared with the exact values (dashed-lines) known from Eq. (19). In all cases,  $L = 1024$ , and averaging is done for  $10^4$  or more samples; data are scaled by factors  $\{\frac{1}{4}, \frac{1}{2}, 1, 2\}$  (bottom to top) for better visibility.

Let  $l$  be the length scale over which coarsening is performed. We define  $\varepsilon_{\mathbf{i}} \equiv \varepsilon_{x,y}$  as the average energy of all the sites belonging to an  $l \times l$  square centered at site  $\mathbf{i} \equiv (x, y)$ ,

$$\varepsilon_{\mathbf{i}} = \frac{1}{l^2} \sum_{m,n=0}^{l-1} H_{x+m,y+n}. \quad (22)$$

The energy spectrum generated by  $\varepsilon_{\mathbf{i}}$  is bounded with an energy gap (difference of consecutive energy values) of  $\mathcal{O}(\frac{1}{l^2})$ . The energy spectrum becomes continuous when  $l$  is large. For our purpose  $l = 8$  turns out right. First we calculate the probability density function  $g(\varepsilon)$  for  $\lambda = 0, -0.1, -0.2$ , which is shown in Fig. 3 (a). Further we define  $n_{\mathbf{i}} = \theta(\varepsilon_{\mathbf{i}} - \varepsilon^*)$  where  $\theta(x)$  is the Heaviside step function that takes the value 0 when  $x$  is negative, and 1 otherwise. Thus,  $n_{\mathbf{i}}$  behaves like the presence and absence of a particle at site  $\mathbf{i}$ . The threshold  $\varepsilon^*$  controls the density of the particles

$$\rho(\varepsilon^*) = \frac{1}{L^2} \sum_{\mathbf{i}} n_{\mathbf{i}} = \int_{\varepsilon^*}^{\infty} g(\varepsilon) d\varepsilon. \quad (23)$$

This is demonstrated in Fig. 3 (b) for  $\lambda = -0.2$ ; the shaded area there represents the particle density  $\rho(\varepsilon^*)$ . A plot of  $\rho(\varepsilon^*)$  is shown in Fig. 3 (c) for different  $\lambda$ .

We are now ready to ask, if the number fluctuations in these point configurations exhibits hyperuniformity. Number of particles in a subsystem of size  $l \times l$  is  $N_l = \sum_{\mathbf{i} \in l \times l} n_{\mathbf{i}}$ .

By construction,  $\langle N_l \rangle = l^2 \rho(\varepsilon^*)$ . We want to calculate the variance,

$$\sigma_{N_l}^2(l) = \langle N_l^2 \rangle - \langle N_l \rangle^2 \sim l^{d-\alpha}. \quad (24)$$

and find out if it scales as  $l^{d-\alpha}$  with  $\alpha$  in the range  $(0, 1)$ . In Fig. 4 (a) we plot  $N_l$  vs  $l$  for a fixed  $\lambda = -0.2$  and different densities  $\rho$ . All of them show the same power-law scaling with  $\alpha = \frac{|a|}{\nu} = 0.432$  (dashed lines), calculated from Eq. (19). Figure 4(b) shows  $\sigma_{N_l}^2(l)$  in log-scale for different values of  $\lambda$  and they exhibit different hyperuniformity exponents, consistent with known values  $\alpha = \frac{|a|}{\nu}$ .

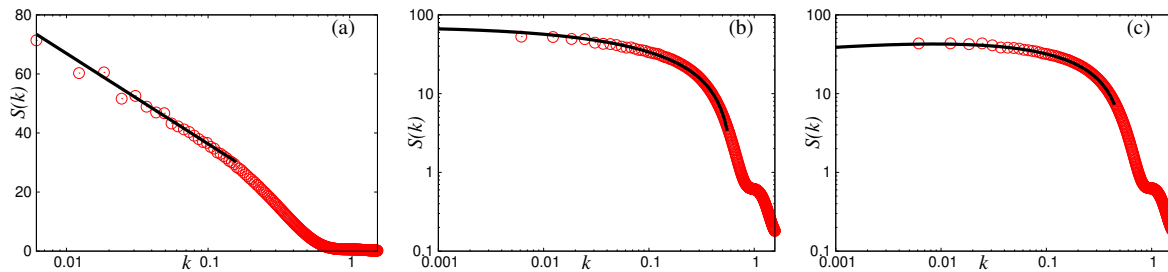


**Figure 5.** Radial structure factor  $S(k)$  as a function of  $k$  for different  $\lambda$  values (symbols) are fitted to the form  $-Ak^\alpha \ln(Bk)$  shown as lines. (a)  $\lambda = 0$  ( $\alpha = 0$ ):  $S(k)$  is plotted with  $x$ -axis in log-scale to see a linear behaviour for small  $k$  that corresponds to  $S(k) \sim \ln(k)$ . (b)  $\lambda = -0.05$  ( $\alpha = 0.123$ ) and (c)  $\lambda = -0.1$  ( $\alpha = 0.236$ ):  $S(k)$  is shown in log-log scale. In all cases  $\varepsilon^*$  is chosen such that  $\rho = \frac{1}{2}$ , and  $S(k)$  is averaged  $10^5$  point configurations.

### 2.3. The structure factor

The structure factor of point configurations generated from the steady-state energy profile of the AT model can be calculated as follows. Given that the exponent  $\alpha$  is independent of particle density, we can choose any particle density. For our calculations, we consider point configurations with a particle density  $\rho(\varepsilon^*) = \frac{1}{2}$  (or  $N = \frac{L^2}{2}$ ) by selecting a suitable  $\varepsilon^*$ . Let  $\mathbf{R}_j$  be the position of the  $j$ -th particle, where  $j = 1, 2, \dots, N$ . The structure factor  $S(\mathbf{k})$  for the point configuration  $\{\mathbf{R}_j\}$  is given by:

$$S(\mathbf{k}) = \left\langle \left| \sum_{j=1}^N e^{i\mathbf{R}_j \cdot \mathbf{k}} \right|^2 \right\rangle = \left\langle \left| \sum_{i \in L \times L} n(\mathbf{r}_i) e^{i\mathbf{r}_i \cdot \mathbf{k}} \right|^2 \right\rangle, \quad (25)$$

where  $\langle \cdot \rangle$  represents the statistical average over the configurations, and  $\mathbf{k} \equiv (k_x, k_y) = \frac{2\pi}{L}(n_x, n_y)$  with  $n_x, n_y = 1, 2, \dots, L$ . The radial form of the structure factor is then:

$$S(k) = \frac{\sum_{\mathbf{k}} S(\mathbf{k}) \delta(k - |\mathbf{k}|)}{\sum_{\mathbf{k}} \delta(k - |\mathbf{k}|)}. \quad (26)$$

For the AT model, point configurations at  $\lambda = -0.05$  and  $\lambda = -0.1$  are expected to have a radial structure factor  $S(k) \sim k^\alpha$  with  $\alpha = 0.123$  and  $\alpha = 0.236$ , respectively, as  $k \rightarrow 0$ . However, it is well known that the structure factor of critical systems in two dimensions does not exhibit pure power laws but contains a multiplicative logarithmic factor, i.e.,  $S(k) \sim k^\alpha \ln k$  [1]. The presence of a strong logarithmic correction can be verified in point configurations of the AT model at  $\lambda = 0$ , where  $\alpha = 0$  and thus  $S(k) \sim \ln(k)$ .

In Fig. 5, we have plotted the radial structure factor  $S(k)$  for  $\lambda = 0, -0.05, -0.1$ . In Fig. 5(a), the plot of  $S(k)$  on a semi-log scale exhibits linearity for small  $k$ , confirming the existence of a strong logarithmic correction. Figures 5 (b) and 5(c) show the same for  $\lambda = -0.05$  and  $\lambda = -0.1$  on a log-log scale. For small  $k$ , the data (symbols) do not show a straight line with a positive slope  $\alpha$ ; the power-law is masked by a strong

logarithmic correction. However, a function of the form  $-Ak^\alpha \ln(Bk)$  (black line) fits the data quite well with  $\alpha = 0.123$  and  $\alpha = 0.236$ , respectively, along with suitable choices of constants  $A$  and  $B$ .

### 3. Conclusion and Discussion

In this article we demonstrate that Ashkin-Teller model on a two dimensional ( $d = 2$ ) square lattice exhibit hyperuniform energy distribution when the inter-spin interaction  $\lambda$  becomes negative: variance of energy of the subsystems of size  $l \times l$  is proportional to  $l^{d-\alpha}$  with  $\alpha = \frac{|a|}{\nu} = d - \frac{2}{\nu}$  where  $\nu, a$  are the correlation length and specific heat exponents respectively. Any point configuration constructed by assigning unity to sites having energy (coarse-grained) exceeding beyond a threshold value, leads to suppressed number fluctuations  $l^{-\alpha}$  across a length scale  $l$ , which vanishes as  $l \rightarrow \infty$ . The exponent  $\alpha = d - \frac{2}{\nu}$  does not depend on the threshold value of energy which controls the particle density of the point configurations.

Besides Ashkin-Teller model several other spin systems exhibit reduced specific heat at their magnetic transition point, as their specific heat exponent  $a$  is negative. Some examples include XY [62] and Heisenberg model [63] in  $d = 3$ , random-field Ising models in  $d = 2$  [64], and  $d = 3$  [65]. There too, one expects to see hyperuniform energy distribution. The advantage in AT model is that here  $\alpha$  varies continuously. This enables us to utilise the steady-state energy configurations of critical Ashkin-teller model to generate real-valued hyperuniform distributions on two dimensional lattices. Using a threshold on a coarse-grained local energy one can also generate hyperuniform particle distribution with any desired exponent and density.

Equilibrium systems exhibit hyperuniform energy distribution when  $0 < \alpha < 1$  or equivalently when  $d\nu > 2$ . This condition is the well-known Harris criterion [66] which states that continuous phase transitions with  $d\nu > 2$  are stable against quenched spatial randomness. This inequality is derived later for systems with uncorrelated point disorder [67]. There are numerous models that obey Harris criteria applies [72], but exceptions do exist [68, 69, 70, 71]. Since systems obeying Harris criteria exhibit hyperuniform energy distribution, one may conjecture that quenched spatial disorder is irrelevant in systems where energy distribution is hyperuniform. Further study is required to establish if such a conjecture is indeed true.

### Acknowledgement

The authors would like to acknowledge helpful discussions with Aikya Banerjee and extend their gratitude to Soumya K Saha for assistance in generating figure 5. PKM gratefully acknowledges the financial support provided by the Science and Engineering Research Board (SERB), Department of Science and Technology, Government of India, under project reference no. MTR/2023/000644 for conducting this research.

## References

- [1] S. Torquato, *Physics Reports* **745**, 1 (2018).
- [2] S. Torquato, *Phys. Rev. E* **94**, 022122 (2016).
- [3] Y. Jiao, T. Lau, H. Hatzikirou, M. Meyer-Hermann, C. C. Joseph, S. Torquato, *Phys. Rev. E* **89**, 022721 (2014).
- [4] A. Barua, A. Beygi, and H. Hatzikirou, *Entropy* **23**, 867 (2021).
- [5] E. Lomba, J. J. Weis, L. Guisández, and S. Torquato, *Phys. Rev. E* **102** 012134 (2020).
- [6] H. Nunley, M. Nagashima, K. Martin, A. L. Gonzalez, S. C. Suzuki, D. A. Norton, R. O. L. Wong, P. A. Raymond, D. K. Lubensky, and D. Umulis, *PLoS. Comput. Biol.* **16**, e1008437 (2020).
- [7] T. Baden and D. Osorio, *Annu. Rev. Vis. Sci.* **5**, 177 (2019)
- [8] Z. Ge, *Proc. Natl. Acad. Sci.* **120**, e2306514120 (2023).
- [9] S. Torquato, *Proc. Natl. Acad. Sci.* **120** e2316879120 (2023).
- [10] L. Dong, *arXiv* 2306.04149 (2023).
- [11] Y. Zheng, L. Liu, H. Nan, Z. X. Shen, G. Zhang, D. Chen, L. He, W. Xu, M. Chen, Y. Jiao, and H. Zhuang, *Sci. Adv.* **6** eaba0826 (2020).
- [12] J. B. Llorens, I. Guillamón, I. G. Serrano, R. Córdoba, J. Sesé, J. M. D. Teresa, M. R. Ibarra, S. Vieira, M. Ortuño, and H. Suderow, *Phys. Rev. Research* **2**, 033133 (2020).
- [13] M. Formanek, S. Torquato, R. Car, and F. Martelli, *J. Phys. Chem. B* **127**, 3946 (2023).
- [14] D. Chen, E. Lomba, and S. Torquato *Phys. Chem. Chem. Phys.* **20**, 17557 (2018).
- [15] Z. Ma, E. Lomba, and S. Torquato, *Phys. Rev. Lett.* **125**, 068002 (2020).
- [16] Y. Gao, Y. Jiao, and Y. Liu, *Phys. Rev. E* **105**, 045305 (2022).
- [17] M. Skolnick and S. Torquato, *Acta Materialia* **250**, 118857 (2023).
- [18] J. Kim and S. Torquato, *Phys. Rev. E* **103**, 012123 (2021).
- [19] G. Zhang, F. H. Stillinger, and S. Torquato, *J. Chem. Phys.* **145**, 244109 (2016).
- [20] J. Wang, J. M. Schwarz, and J. D. Paulsen, *Nat. Commun.* **9**, 2836 (2018).
- [21] M. Basu, U. Basu, S. Bondyopadhyay, P. K. Mohanty, and H. Hinrichsen, *Phys. Rev. Lett.* **109**, 015702 (2012).
- [22] D. Hexner and D. Levine, *Phys. Rev. Lett.* **114**, 110602 (2015).
- [23] Y. Zheng, A. D. S. Parmar, and M. P. Ciamarra, *Phys. Rev. Lett.* **126**, 118003 (2021).
- [24] P. Grassberger, D. Dhar, and P. K. Mohanty *Phys. Rev. E* **94**, 042314 (2016).
- [25] S. Goldstein, J. L. Lebowitz, E. R. Speer, *arXiv* 2401.16505 (2024).
- [26] G. Zhang, F. Martelli, and S. Torquato, *J. Phys. A: Math. Theor.* **51**, 115001 (2018).
- [27] S. Torquato, G. Zhang and M. de Courcy-Ireland *J. Stat. Mech.* 093401 (2018).
- [28] M. A. Klatt and S. Torquato, *Phys. Rev. E* **94**, 022152 (2016).
- [29] T. M. Middlemas, F. H. Stillinger, and S. Torquato, *Phys. Rev. E* **99**, 022111 (2019).
- [30] E. C. Oğuz, J. E. S. Socolar, P. J. Steinhardt, and S. Torquato, *Phys. Rev. B* **95**, 054119 (2017).
- [31] M. Björklund, and T. Hartnick, *Math. Ann.* **389**, 365 (2024).
- [32] D. Chen, H. Zhuang, M. Chen, P. Y. Huang, V. Vlcek, Y. Jiao, *Appl. Phys. Rev.* **10**, 021310 (2023).
- [33] N. Zhang , C. Gao , and Y. Xiong , *J. Energy Chem.* **37**, 43 (2019).
- [34] Z. Shi , M. Li , J. Sun , and Z. Chen , *Adv. Energy Mater.* **11**, 2100332 (2021).
- [35] R. Dandekar, *EPL* **132**, 10008 (2020).
- [36] Q. Lei,; R. Ni, *Proc. Natl. Acad. Sci.* **116** (46), 22983 (2019).
- [37] H. Fischer, *A History of the Central Limit Theorem: From Classical to Modern Probability Theory*, Springer, New York (2011).
- [38] J. Cardy, *Scaling and Renormalization in Statistical Physics*, Cambridge University Press (1996).
- [39] L.S. Ornstein, F. Zernike, Accidental deviations of density and opalescence at the critical point of a single substance, *Proc. Akad. Sci.* **17**, 793 (1914).
- [40] P. Attard, *Thermodynamics and Statistical Mechanics*, Academic Press Inc, London (2008).
- [41] J. P. Hansen and I. R. McDonald, *Theory of Simple Liquids*, Academic Press, New York (1986).

- [42] S. Torquato, F. H. Stillinger, *Phys. Rev. E* **68**, 041113 (2003).
- [43] S. S. Manna, *J. Phys. A: Math. Gen.* **24**, L363 (1991).
- [44] L. Galliano, M. E. Cates, and L. Berthier, *Phys. Rev. Lett.* **131**, 047101 (2023).
- [45] M. Henkel, H. Hinrichsen, and S. Lübeck, *Non-Equilibrium Phase Transitions*, Vol. 1, Springer, Berlin (2008).
- [46] V. Frette, *Phys. Rev. Lett.* **70**, 2762 (1993).
- [47] K. Christensen, A. Corral, V. Frette, J. Feder, and T. Jossang, *Phys. Rev. Lett.* **77**, 107 (1996).
- [48] M. Rossi, R. Pastor-Satorras, and A. Vespignani, *Phys. Rev. Lett.* **85**, 1803 (2000).
- [49] E. Tjhung and L. Berthier, *Phys. Rev. Lett.* **114**, 148301 (2015).
- [50] U. Basu, P. K. Mohanty, *Phys. Rev. E* **79** (4), 041143 (2009).
- [51] Y. Lei1 and R. Nil, *arXiv* 2405.12818 (2024).
- [52] J. Ashkin and E. Teller, *Phys. Rev.* **64**, 178 (1943).
- [53] F. Y. Wu and K.Y. Lin, *J. Phys. C* **7**, L181 (1974).
- [54] L. P. Kadanoff, *Phys. Rev. Lett.* **39**, 903 (1977).
- [55] R. J. Baxter, *Exactly Solved Model in Statistical Mechanics*, Academic Press, London (1982).
- [56] F. J. Wegner, *J. Phys. C: Solid State Phys.* **5**, L131 (1972).
- [57] R. J. Baxter, *Ann. Phys. (NY)* **70**, 193 (1972).
- [58] M. Suzuki, *Prog. Theor. Phys.* **51**, 1992 (1974).
- [59] E. A. Guggenheim, *Chem. Phys.* **13**, 253 (1945).
- [60] C. H. Back, Ch. Würsch, A. Vaterlaus, U. Ramsperger, U. Maier, and D. Pescia, *Nature* **378**, 597 (2005).
- [61] I. Mukherjee, P. K. Mohanty *Phys. Rev. B* **108**, 174417 (2023).
- [62] A. P. Gottlob, M. Hasenbusch, *Physica A* **201**, 593 (1993).
- [63] C. Holm, W. Janke, *Phys. Rev. B* **48**, 936 (1993).
- [64] A. K. Hartmann and A. P. Young, *Phys. Rev. B* **64**, 214419 (2001).
- [65] H. Rieger and A. P. Young, *J. Phys. A: Math. Gen.* **26**, 5279 (1993).
- [66] A. B. Harris, *J. Phys. C* **7**, 1671 (1974).
- [67] J. T. Chayes, L. Chayes, D. S. Fisher, and T. Spencer, *Phys. Rev. Lett.* **57**, 2999 (1986).
- [68] R. R. P. Singh and M. E. Fisher, —it *Phys. Rev. Lett.* **60**, 548 (1988).
- [69] H. R. Cruz and R. B. Stinchcombe, *J. Phys. C: Solid State Phys.* **19**, 3555 (1986).
- [70] M. Schrauth, J. S. E. Portela, and F. Goth, *Phys. Rev. Lett.* **121**, 100601 (2018).
- [71] S. Fayfar, A. Bretaña, and W. Montfrooij, *Phys. Rev. E* **104**, 034110 (2021).
- [72] H. A. Brooks, *J. Phys: Condens. Matter* **28** 421006 (2016).